

# Inhibition of Hypothalamic Inflammation Reverses Diet-Induced Insulin Resistance in the Liver

Marciane Milanski,<sup>1,2</sup> Ana P. Arruda,<sup>1</sup> Andressa Coope,<sup>1</sup> Letícia M. Ignacio-Souza,<sup>1</sup> Carla E. Nunez,<sup>1</sup> Erika A. Roman,<sup>1</sup> Talita Romanatto,<sup>1</sup> Livia B. Pascoal,<sup>1</sup> Andrea M. Caricilli,<sup>3</sup> Marcio A. Torsoni,<sup>1,2</sup> Patricia O. Prada,<sup>2</sup> Mario J. Saad,<sup>3</sup> and Licio A. Velloso<sup>1</sup>

Defective liver gluconeogenesis is the main mechanism leading to fasting hyperglycemia in type 2 diabetes, and, in concert with steatosis, it is the hallmark of hepatic insulin resistance. Experimental obesity results, at least in part, from hypothalamic inflammation, which leads to leptin resistance and defective regulation of energy homeostasis. Pharmacological or genetic disruption of hypothalamic inflammation restores leptin sensitivity and reduces adiposity. Here, we evaluate the effect of a hypothalamic anti-inflammatory approach to regulating hepatic responsiveness to insulin. Obese rodents were treated by intracerebroventricular injections, with immunoneutralizing antibodies against Toll-like receptor (TLR) 4 or tumor necrosis factor (TNF) $\alpha$ , and insulin signal transduction, hepatic steatosis, and gluconeogenesis were evaluated. The inhibition of either TLR4 or TNF $\alpha$  reduced hypothalamic inflammation, which was accompanied by the reduction of hypothalamic resistance to leptin and improved insulin signal transduction in the liver. This was accompanied by reduced liver steatosis and reduced hepatic expression of markers of steatosis. Furthermore, the inhibition of hypothalamic inflammation restored defective liver glucose production. All these beneficial effects were abrogated by vagotomy. Thus, the inhibition of hypothalamic inflammation in obesity results in improved hepatic insulin signal transduction, leading to reduced steatosis and reduced gluconeogenesis. All these effects are mediated by parasympathetic signals delivered by the vagus nerve. *Diabetes* 61:1455–1462, 2012

**D**efective liver gluconeogenesis is regarded as the main mechanism leading to fasting hyperglycemia in type 2 diabetes and, in concert with steatosis, is the hallmark of hepatic insulin resistance (1,2). Both clinical and experimental data support an early link between obesity, hepatic insulin resistance, and hyperglycemia (3), which places this specific defect in a strategic position as a target for the treatment of type 2 diabetes (4,5). The relevance of tackling gluconeogenesis for the treatment of type 2 diabetes can be illustrated by the therapeutic success of metformin, a drug widely used for >50 years, whose molecular mechanism of action recently has been described (6).

From the <sup>1</sup>Laboratory of Cell Signaling, University of Campinas, Campinas, Brazil; the <sup>2</sup>Faculty of Applied Sciences, University of Campinas, Campinas, Brazil; and the <sup>3</sup>Department of Internal Medicine, University of Campinas, Campinas, Brazil.

Corresponding author: Licio A. Velloso, lavelloso.unicamp@gmail.com.

Received 22 March 2011 and accepted 6 February 2012.

DOI: 10.2337/db11-0390

This article contains Supplementary Data online at <http://diabetes.diabetesjournals.org/lookup/suppl/doi:10.2337/db11-0390/-/DC1>.

M.M. and A.P.A. contributed equally to this article.

© 2012 by the American Diabetes Association. Readers may use this article as long as the work is properly cited, the use is educational and not for profit, and the work is not altered. See <http://creativecommons.org/licenses/by-nc-nd/3.0/> for details.

See accompanying commentary, p. 1350.

A number of recent studies have shown that experimental obesity results from the installation of an inflammatory process in the hypothalamus, which leads to resistance to the anorexigenic hormones leptin and insulin and finally to the defective regulation of food intake and energy expenditure (7–12). Although the development of increased adiposity is taken as the main outcome of hypothalamic dysfunction, connecting obesity to type 2 diabetes, other peripheral functions can be controlled by the hypothalamus and play an important role in the development or progression of the hyperglycemic phenotype (13). One such example is the neural control of gluconeogenesis that depends on the adequate functionality of the insulin and AMP-activated protein kinase (AMPK) signaling pathways in hypothalamic neurons (14), which can be disturbed by drug-induced endoplasmic reticulum stress and inflammation, generating a sympathetic signal that triggers hepatic insulin resistance (15). Both the genetic and pharmacological approaches used to modulate both these pathways in the hypothalamus were able to affect liver gluconeogenesis (16).

Here, we explore the hypothesis that hepatic gluconeogenesis and hepatic insulin resistance can be corrected by reducing diet-induced hypothalamic inflammation. Our results show that the inhibition of either TLR4 or TNF $\alpha$  signaling in the hypothalamus improves insulin signal transduction in the liver and reduces hepatic glucose production.

## RESEARCH DESIGN AND METHODS

The experimental procedures involving rats and mice were performed in accordance with the guidelines of the Brazilian College for Animal Experimentation and were approved by the ethics committee at the State University of Campinas. Male Wistar rats, male TNFRp55<sup>-/-</sup> or TNFRp55<sup>+/-</sup> mice (knockout for the TNF $\alpha$  receptor 1 and its respective control) (17), male C3H/HeJ or C3H/HeN mice (loss-of-function mutation for TLR4 and its respective control) (18), and male LDLR-KO mice (knockout for the LDL receptor) (19) were fed standard rodent chow or a high-fat diet (see composition in Supplementary Table 1) for 8 weeks and then stereotaxically instrumented using a Stoelting stereotaxic apparatus, according to a previously described method (20). Cannula efficiency was tested 1 week after cannulation by the evaluation of the drinking response elicited by intracerebroventricular angiotensin II. Stereotaxic coordinates were, for rats, anteroposterior, 0.2 mm lateral, 1.5 mm depth, and 4.0 mm and for mice, anteroposterior, 0.34 mm lateral, 1.0 mm depth, and 2.2 mm. Thereafter, rats or mice were intracerebroventricularly treated with an anti-TLR4 antibody (50 ng twice a day TLR4 sc13591; Santa Cruz Biotechnology, Santa Cruz, CA) or the anti-TNF $\alpha$  monoclonal antibody, infliximab (0.3  $\mu$ g twice a day), for 7 days. During the experimental period, the experimental animals had access to their respective diets and to water ad libitum and were housed at 22°C with a 12-h light/dark cycle. In some experiments, lean TNFRp55<sup>-/-</sup>, TNFRp55<sup>+/-</sup>, C3H/HeJ, or C3H/HeN mice were intracerebroventricularly treated with 2  $\mu$ L stearic acid (90  $\mu$ mol/L) twice a day for 5 days. Fatty acid salt solution was added to medium containing fatty acid-free BSA (Sigma) for 1 h of conjugation at 37°C with continuous agitation to avoid precipitation. The fatty acid-to-BSA molar ratio was 3 to 1.

**Diet composition.** The chow and high-fat diet were evaluated for the content of fatty acids by chromatography, as previously described (21).

**Liver histology.** Hydrated 5- $\mu$ m sections of paraformaldehyde-fixed, paraffin-embedded liver specimens were stained by regular hematoxylin-eosin methodology for evaluation of liver histology.

**Glucose tolerance test.** After a 12-h fast, 2.0 g/kg i.p. glucose was administered, and blood samples were obtained from the cut tip of the tail 0, 30, 60, and 120 min later for the determination of serum glucose and insulin concentrations. The glucose and insulin responses during the glucose tolerance test were calculated by estimating the total area under the glucose curve, using the trapezoidal method (22).

**Pyruvate tolerance test.** After a 16-h fast, 2.0 g/kg i.p. pyruvate was administered, and blood samples were obtained from the cut tip of the tail 0, 15, 30, 60, 90, and 120 min later for the determination of serum glucose concentration. The glucose responses during the pyruvate tolerance test were calculated by estimating the total area under the glucose curve, using the trapezoidal method (22).

**Hyperinsulinemic-euglycemic clamp.** Food was removed 12 h before the beginning of in vivo studies, the intracerebroventricularly cannulated rats were anesthetized with sodium pentobarbital (50 mg/kg body wt) injected intraperitoneally, and catheters were then placed into the left jugular vein (for tracer infusions) and carotid artery (for blood sampling), as previously described (23). A prime continuous insulin infusion at a rate of 3.6 mU/kg body wt/min was performed to raise the plasma insulin concentration to ~800–900 pmol/L. Blood samples (20  $\mu$ L) were collected at 5-min intervals for the immediate measurement of plasma glucose concentration, and 10% unlabeled glucose was infused at variable rates to maintain plasma glucose at fasting levels. Insulin-stimulated whole-body glucose flux was estimated using a prime continuous infusion of high-performance liquid chromatography-purified [ $^3$ -H] glucose (10  $\mu$ Ci bolus, 0.1  $\mu$ Ci/min) throughout the clamp procedure. Blood samples (10  $\mu$ L) were collected before the start and during the glucose infusion period (every 30 min) for measurement of plasma insulin concentrations. All infusions were performed using Harvard infusion pumps. At the end of the clamp procedure, the animals were killed by a sodium pentobarbital intravenous injection. In separate experiments, glucose turnover basal rates were measured by continuously infusing [ $^3$ -H] glucose (0.02  $\mu$ Ci/min) for 120 min. Blood samples (20  $\mu$ L) were collected at 100, 110, and 120 min after the start of the experiment to determine plasma [ $^3$ -H] glucose concentration.

**Immunoblotting.** Liver, hypothalamus, and soleus muscle specimens were homogenized by sonication (15 s) in an antiprotease cocktail (10 mmol/L imidazole, pH 8.0; 4 mmol/L EDTA; 1 mmol/L EGTA; 0.5 g/L pepstatin A; 2 g/L aprotinin; 2.5 mg/L leupeptin; 30 mg/L trypsin inhibitor; 200  $\mu$ mol/L DL-dithiothreitol; and 200  $\mu$ mol/L phenylmethylsulfonyl fluoride). After sonication, an aliquot of extract was collected and the total protein content was determined by the dye-binding protein assay kit (Bio-Rad Laboratories, Hercules, CA). Samples containing 50–125  $\mu$ g of protein from each experimental group were incubated for 5 min at 80°C with four-times-concentrated Laemmli sample buffer (1 mmol sodium phosphate/L, pH 7.8; 0.1% bromophenol blue; 50% glycerol; 10% SDS; and 2% mercaptoethanol) or immunoprecipitated (1.0 mg of protein) with anti-IR or anti-IRS1 (4:1, vol/vol) and then run on 10% polyacrylamide gels at 120 V for 30 min. Electrotransfer of proteins to nitrocellulose membranes (Bio-Rad) was performed for 1 h at 120 V (constant) in buffer containing methanol and SDS. After checking the efficiency of transfer by staining with Ponceau S, the membranes were blocked with 5% skimmed milk in Tween-Tris-buffered saline (TTBS) (10 mmol Tris/L, 150 mmol NaCl/L, and 0.5% Tween 20) overnight at 4°C. Fatty acid synthase (FAS), peroxisome proliferator-activated receptor (PPAR)  $\gamma$  coactivator (PGC) 1 $\alpha$ , PPAR $\alpha$ , phosphorylated protein kinase B (pAkt), phosphorylated forkhead box protein O1 (pFOXO), phosphorylated inhibitor of nuclear factor kappa B-alpha (pIKB $\alpha$ ), inhibitor of nuclear factor kappa B-alpha (IKB $\alpha$ ), and *p*-tyrosine were detected in the membranes after a 2-h incubation at room temperature with primary antibodies (FAS sc20140, PPAR $\alpha$  sc9000, pAkt sc7985-R, pTyr sc508, IR $\beta$  sc711, IRS1 sc560, IRS2 sc1556, pIKB $\alpha$  sc52943, and IKB $\alpha$  sc56710 [Santa Cruz Biotechnology] and pFOXO no. 9464 L and PGC1 no. 4259S [Cell Signaling]) (diluted 1:500 in TTBS containing 3% dry skimmed milk). The membranes were then incubated with a secondary specific immunoglobulin G antibody (diluted 1:5,000 in TTBS containing 3% dry skimmed milk) for 2 h at room temperature. Enhanced chemiluminescence (SuperSignal West Pico; Pierce) after incubation with a horseradish peroxidase-conjugated secondary antibody was used for detection by autoradiography. Band intensities were quantified by optical densitometry (Scion Image, Frederick, MD).

**Real-time PCR.** The expressions of TNF $\alpha$ , interleukin (IL)-1 $\beta$ , IL-6 (hypothalamus and other brain regions), PEPCK, and G6Pase (liver) mRNAs were measured in samples obtained from rats or mice treated intracerebroventricularly with an anti-TLR4 antibody or the anti-TNF $\alpha$  monoclonal antibody, infliximab, or fed a high-fat diet only. Intron-skipping primers were obtained from Applied Biosystems. Glyceraldehyde-3-phosphate dehydrogenase (GAPDH) primers were used as controls. The endogenous control for normalization of GAPDH was hypoxanthine-guanine phosphoribosyl transferase. No significant

change in GAPDH expression was detected in the different experimental conditions. Real-time PCR analysis of gene expression was performed using an ABI Prism 7500 sequence detection system (Applied Biosystems). The optimal concentration of cDNA and primers, as well as the maximum efficiency of amplification, was obtained through five-point, twofold dilution curve analysis for each gene. Each PCR contained 20 ng of reverse-transcribed RNA and was run according to the manufacturer's recommendation using the TaqMan PCR Master Mix (Applied Biosystems). Real-time data were analyzed using the Sequence Detector System 1.7 (Applied Biosystems).

**Vagotomy.** The surgical procedure for vagotomy was performed simultaneously with the stereotaxic instrumentation. For this, rats were anesthetized with sodium pentobarbital (50 mg/kg i.p.). The stomach and lower esophagus were exteriorized from the peritoneal cavity and wrapped in cotton moistened with saline. The common hepatic branch of the ventral vagal trunk and the accessory celiac and gastric branches of the ventral vagal trunk and dorsal vagal trunk were transected. Experiments were started after 1 week, when the rats were fully recovered.

**Inhibition of parasympathetic activity with olanzapine.** In some experiments, rats were treated with 0.5 mg/kg i.p. of the antimuscarinic agent olanzapine, twice a day for 7 days (24). This treatment was performed in parallel with the intracerebroventricular treatments with either anti-TLR4 antibody or infliximab.

**Statistical analysis.** Results are presented as means  $\pm$  SE. The Levene test for the homogeneity of variances was initially used to check the fit of data to the assumptions for parametric ANOVA. To correct for variance heterogeneity or nonnormality, data were log transformed. All results were analyzed by one-way ANOVA. When necessary, these analyses were complemented by the Tukey test to determine the significance of individual differences. The level of significance was set at  $P < 0.05$ . Data were analyzed using the Statistic Software package (StatSoft, Tulsa, OK).

## RESULTS

**The inhibition of TLR4 and TNF $\alpha$  in the hypothalamus reduces hypothalamic inflammation and corrects leptin resistance.** The consumption of a high-fat diet produces a hypothalamus-restricted inflammation in the central nervous system (Fig. 1A). The short-term intracerebroventricular treatment with an antiserum that inhibits TLR4 and an anti-TNF $\alpha$  monoclonal antibody significantly reduces the expressions of TNF $\alpha$ , IL-1 $\beta$ , and IL-6 in the hypothalamus of obese rats (Fig. 1B). This is accompanied by the inhibition of nuclear factor  $\kappa$ B, as determined by the phosphorylation/expression of the inhibitory protein IKB $\alpha$  (Fig. 1C). These effects are accompanied by a complete correction of hypothalamic leptin resistance, as determined by the leptin-induced reduction of food intake (Fig. 1D). In addition, TLR4, but not TNF $\alpha$ , inhibition produces a significant reduction in body mass (Fig. 1E).

**The inhibition of TLR4 and TNF $\alpha$  in the hypothalamus restores glucose homeostasis in obese rats and improves insulin signal transduction in the liver but not skeletal muscle.** The intracerebroventricular injection of an inhibiting TLR4 antiserum or an anti-TNF $\alpha$  monoclonal antibody corrects obesity-associated glucose intolerance, as determined by an intraperitoneal glucose tolerance test (Fig. 1F and G). This is accompanied by the reversal of diet-induced defective insulin signal transduction through the insulin receptors IRS1, IRS2, Akt, and FOXO1 in the liver and only of the insulin signaling through IRS1 in skeletal muscle (Fig. 1H and I).

**Inhibition of diet-induced hypothalamic inflammation corrects liver steatosis and defective gluconeogenesis.** As depicted in Fig. 2A and B, the inhibition of hypothalamic TLR4 and TNF $\alpha$  results in an almost complete restoration of the liver macroscopic aspect to a lean phenotype, resuming a reddish color instead of the yellowish color exhibited by obese rats (Fig. 1A). The reduction of liver fat deposition in anti-TLR4- and anti-TNF $\alpha$ -treated rats is further confirmed by histological evaluation (Fig. 2B) and determination of liver triglyceride content (Fig. 2C). This is

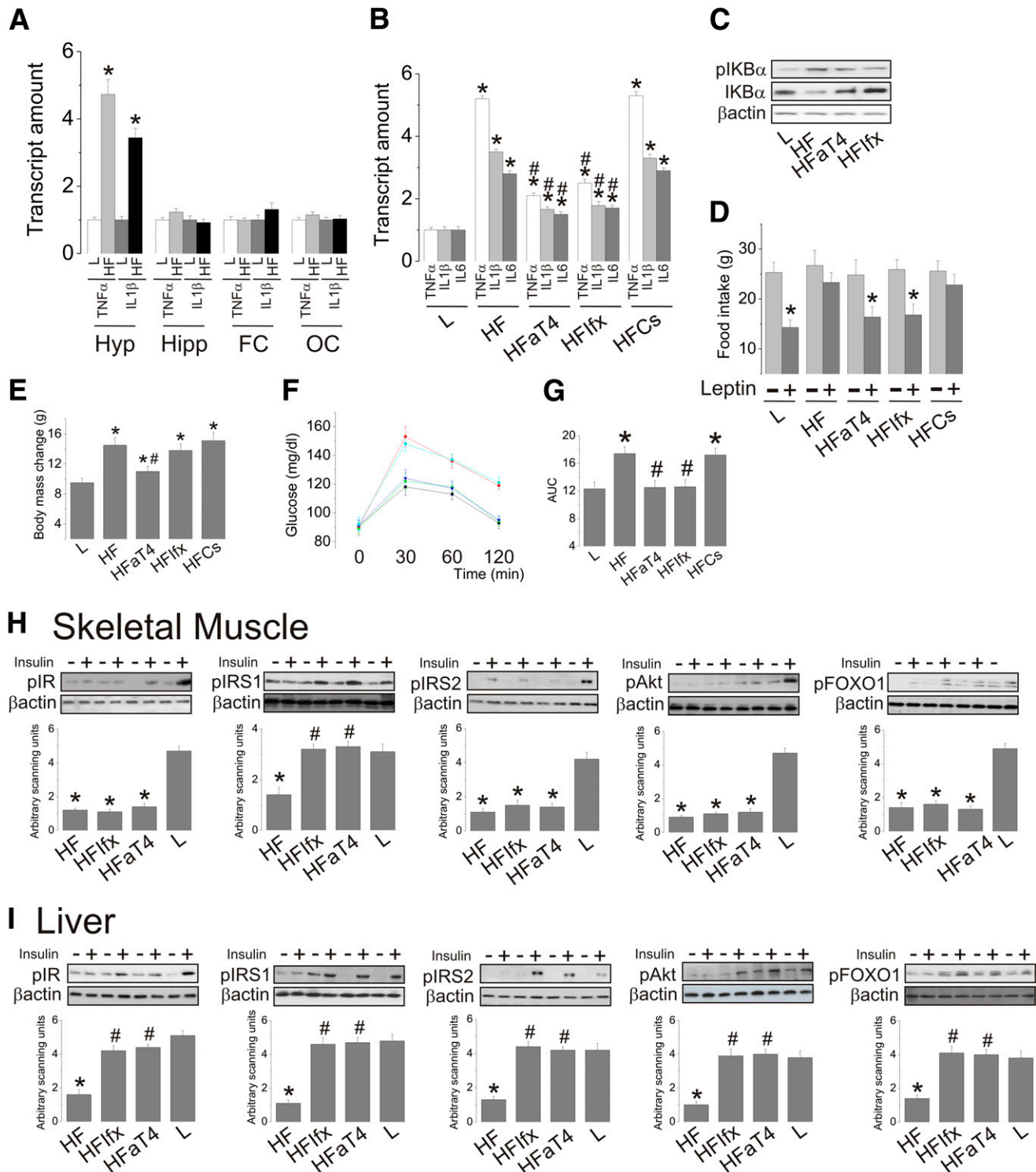


**FIG. 1.** The effect of intracerebroventricular inhibition of TLR4 and TNF $\alpha$  on hypothalamic inflammation, glucose homeostasis, and peripheral insulin sensitivity. **A:** Gene expression of TNF $\alpha$  and IL-1 $\beta$  were determined by real-time PCR in the hypothalamus (Hyp), hippocampus (Hipp), frontal (FC), and occipital (OC) cortices of lean (L) and diet-induced obese (HF) rats. ICV-cannulated lean rats were treated with 2.0  $\mu$ L saline (L); diet-induced obese rats were treated with 2.0  $\mu$ L saline (HL), or anti-TLR4 antibody (50 ng in 2.0  $\mu$ L [HFaT4]), or anti-TNF $\alpha$  monoclonal antibody infliximab (0.3  $\mu$ g in 2.0  $\mu$ L [HFIfx]), or serum without antibody (high-fat diet controls [HFCs]) twice a day for 7 days. **B:** Gene expressions of TNF $\alpha$ , IL-1 $\beta$ , and IL-6 in the hypothalamus assessed by real-time PCR. **C:** The expression of phospho-IKB $\alpha$  (pIKB $\alpha$ ) and total IKB $\alpha$  was determined by immunoblot. **D:** Food intake during 12 h after injection of 2.0  $\mu$ L leptin ( $10^{-6}$ ). **E:** Body mass change during the intracerebroventricular treatment. **F:** Intraperitoneal glucose tolerance test and respective areas under the curve of glucose. **H** and **I:** The rats were anesthetized and submitted to a venous (cava vein) injection of saline (-) or insulin (+) (100  $\mu$ L,  $10^{-6}$  mol/L). Samples of skeletal muscle (**H**) and liver (**I**) were used for the determination of insulin-induced tyrosine phosphorylation of IR $\beta$ , IRS1, and IRS2 and serine phosphorylation of Akt and FOXO1. IR $\beta$ , IRS1, and IRS2 tyrosine phosphorylation were evaluated in total protein extracts submitted to immunoprecipitation with anti-IR $\beta$ , anti-IRS1, or anti-IRS2 antibodies and immunoblotted with anti-phosphotyrosine antibodies. Data are means  $\pm$  SE. In all except **D**, \* $P$  < 0.05 vs. lean (L); # $P$  < 0.05 vs. obese (HF). **D:** \* $P$  < 0.05 vs. respective leptin untreated (-) group. **A** and **B:**  $n$  = 5 rats. **C-I:**  $n$  = 6–8 rats. **F:** Black, L; red, HL; green, HFaT4; blue, HFIfx; cyan, HFCs. (A high-quality color representation of this figure is available in the online issue.)

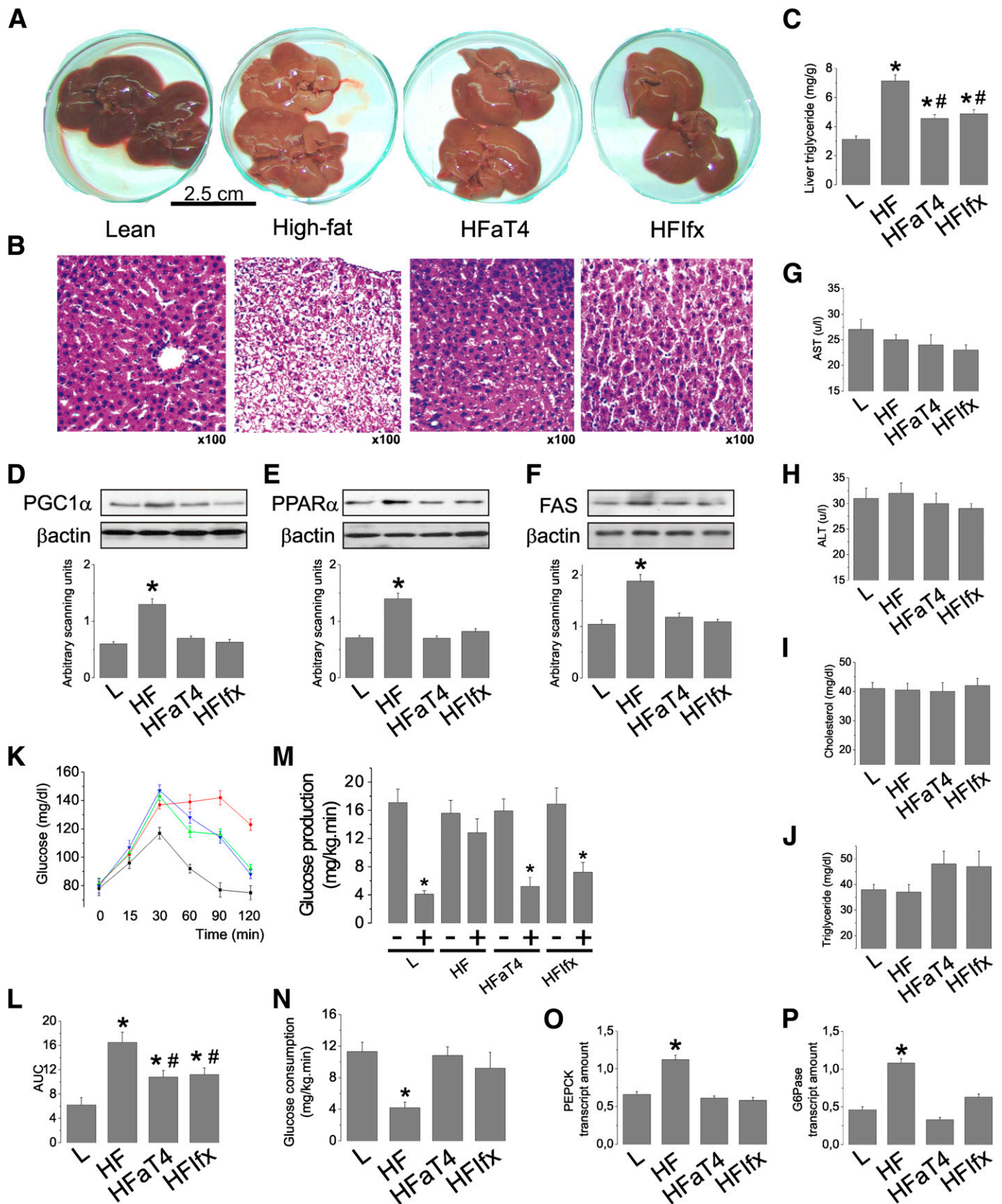


**FIG. 2.** The effect of hypothalamic inflammation inhibition on liver parameters. Intracerebroventricularly cannulated lean rats were treated with 2.0  $\mu$ L saline (L); diet-induced obese rats were treated with 2.0  $\mu$ L saline (HF) or anti-TLR4 antibody (50 ng in 2.0  $\mu$ L [HFaT4]) or anti-TNF $\alpha$  monoclonal antibody infliximab (0.3  $\mu$ g in 2.0  $\mu$ L [HFifx]) twice a day for 7 days. **A:** Macroscopic aspect of the liver in response to 7 days of treatment. **B:** Histological analysis of liver stained with hematoxylin and eosin, representative of five independent experiments. **C:** Liver triglyceride concentration. **D-F:** PGC1 $\alpha$  (D), PPAR $\alpha$  (E), and FAS (F) protein levels in liver assessed by immunoblotting. **G-J:** Blood levels of AST (G), ALT (H), cholesterol (I), and triglycerides (J). **K and L:** Blood glucose levels (K) and respective areas under the curve (L) during the test. **M:** Glucose production (mg/kg.min) in response to insulin. - indicates no insulin, + indicates insulin. **N:** Glucose consumption (mg/kg.min). **O:** PEPCK transcript amount. **P:** G6Pase transcript amount. \* p < 0.05 vs L; # p < 0.05 vs HF.

accompanied by the complete restoration of the hepatic expression of proteins involved in lipogenesis (PGC1 $\alpha$ , PPAR $\alpha$ , and FAS) (Fig. 2D–F). Although the diet and the hypothalamic inhibition of TLR4 and TNF $\alpha$  produced no significant changes in the blood levels of aspartate aminotransferase (AST), alanine aminotransferase (ALT), cholesterol, and triglycerides (Fig. 2G–J), it is interesting to note that blood triglyceride levels presented a tendency to increase in the experimental animals submitted to the anti-inflammatory approach, suggesting an increased mobilization of fat in the liver (Fig. 2J). In addition, the inhibition of hypothalamic inflammation significantly reduced the glucose area under the curve during the pyruvate tolerance test (Fig. 2K and L) and reduced hepatic glucose production (Fig. 2M) and whole-body glucose consumption (Fig. 2N) during the hyperinsulinemic-euglycemic clamp. These outcomes were accompanied by a reduction in the expression of the gluconeogenic enzymes PEPCK and G6Pase (Fig. 2O and P).

**Vagotomy and pharmacological inhibition of muscarinic receptors reverse the beneficial effects of the anti-inflammatory approach in the hypothalamus upon hepatic function.** Vagotomy almost completely reverses the effects of the inhibition of TLR4 and TNF $\alpha$  in the hypothalamus upon liver fat deposition, as demonstrated by histological analysis (Fig. 3A). This is accompanied by a reversal of the effect of the anti-inflammatory approach in the hypothalamus on hepatic insulin signal transduction through IR, IRS1, Akt, and FOXO1 (Fig. 3B) by restoration of the glucose area under the curve during the pyruvate tolerance test (Fig. 3C and D) and by restoration of the hepatic glucose production during a hyperinsulinemic-euglycemic clamp (Fig. 3E). Finally, all these findings are accompanied by vagotomy-related reversal of the anti-inflammatory hypothalamic approach on the hepatic expressions of PEPCK and G6Pase (Fig. 3F and G). As the vagus nerve provides parasympathetic/cholinergic innervation to the liver, we evaluated the effect of an antimuscarinic drug, olanzapine, on the hypothalamic anti-inflammatory activity of the anti-TLR4 antibody and infliximab. The use of olanzapine alone was not capable of reducing diet-induced inflammation of the hypothalamus (not shown). However, when used simultaneously with either the anti-TLR4 antibody or infliximab, it completely opposes the protective effects of the hypothalamic anti-inflammatory approach on liver insulin signal transduction through IR, IRS1, and Akt (Fig. 3H).

**TLR4 loss-of-function mutants and TNF $\alpha$  receptor 1 knockout mice are protected from hypothalamic stearic acid-induced liver insulin resistance.** LR4 loss-of-function mutants and TNF $\alpha$  receptor 1 knockout mice are protected from diet-induced hepatic insulin resistance, as evaluated by insulin signal transduction through IR, IRS1, and Akt (Fig. 3I) and as previously published (17,18). To further explore the roles of hypothalamic TLR4 and TNF $\alpha$  activity on hepatic insulin resistance, lean mice were treated intracerebroventricularly with a long-chain saturated fatty acid, according to a protocol previously published (10). Five days of injection of stearic acid intracerebroventricularly induces hypothalamic inflammation

without affecting systemic inflammatory markers (25). As depicted in Fig. 3J, although control mice and C3H/HeN and TNFRp55<sup>+/+</sup> mice exhibited clear evidence of hepatic insulin resistance following stearic acid intracerebroventricularly, loss-of-function TLR4 mutants and TNFRp55<sup>-/-</sup> mice were completely protected from this effect.

**LDL receptor knockout mice present improved insulin signal transduction following intracerebroventricular anti-TLR4 antibody and infliximab injections even in the presence of sustained expression of markers of hepatic steatosis.** In Wistar rats, the hypothalamic inhibition of either TLR4 or TNF $\alpha$  signaling resulted in the simultaneous reduction of steatosis and improvement of insulin action. To evaluate if the resulting reduction of hepatic insulin resistance was a primary outcome or a consequence of the reduction of steatosis, we treated high-fat-fed LDL receptor knockout mice with intracerebroventricular injections of either the anti-TLR4 antibody or infliximab and evaluated hepatic insulin signaling. The LDL receptor knockout mouse develops an early hepatic steatosis that is resistant to most therapeutic approaches. In contrast to Wistar rats (Fig. 2D–F), obese LDL receptor knockout mice presented no reduction of the expression of markers of steatosis, such as PGC1 $\alpha$  and PPAR $\alpha$  (Fig. 3K). Nevertheless, the inhibition of hypothalamic inflammation resulted in improvement of hepatic insulin signal transduction through IR and IRS1 (Fig. 3L).

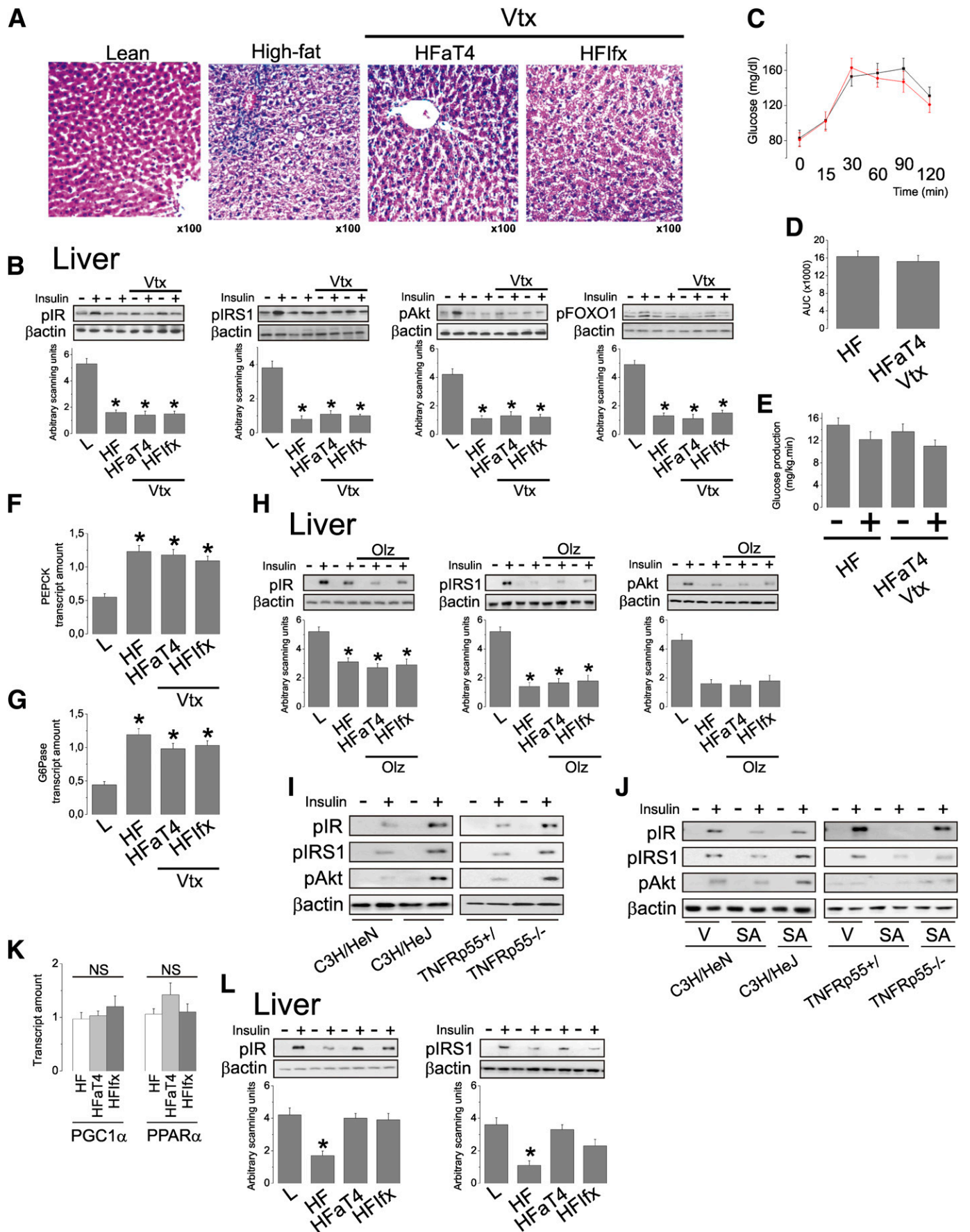
## DISCUSSION

The precise regulation of hepatic gluconeogenesis plays a major role in the maintenance of whole-body glucose homeostasis. Under physiological conditions, hormones, nutrients, and neural signals act in concert to avoid broad oscillations in the blood levels of glucose. However, as insulin action is fundamental for this process, the development of insulin resistance in the liver is accompanied by a progressive deterioration of the control of hepatic glucose production.

Over the last decade, great advances have been made in the characterization of the molecular mechanisms involved in the control of hepatic gluconeogenesis. This was achieved thanks to the identification of the main molecular targets for the action of insulin and glucagon in the liver. In addition, a number of studies have expanded our knowledge on the neural circuits regulating hepatic glucose production. The activation of an ATP-sensitive K<sup>+</sup> channel in medio-basal hypothalamic neurons provides a gluconeogenesis-inhibiting signal that is conveyed to the liver by parasympathetic vagal fibers (26). Because the neurons involved in this process are responsive to leptin and insulin, hypothalamic resistance to these hormones potentially affects the control of hepatic glucose production (27,28).

Hypothalamic resistance to leptin and insulin has been detected in a number of animal models of obesity (29,30). In fact, in one study, the installation of insulin resistance in the hypothalamus was shown to precede liver and adipose tissue resistance to this hormone (23), placing the

pyruvate tolerance test. *M* and *N*: Hepatic glucose production (*M*) and whole-body glucose consumption (*N*) during the hyperinsulinemic-euglycemic clamp, performed at the end of 7 days of treatment. *O* and *P*: PEPCK (*O*) and G6Pase (*P*) mRNA levels in liver, assessed by real-time PCR. Data are means  $\pm$  SE. In all except *M*, \**P* < 0.05 vs. lean (L); #*P* < 0.05 vs. diet-induced obese (HF). *M*: \**P* < 0.05 vs. respective insulin untreated (-). In all experiments, *n* = 5–8 animals. *K*: Black, *L*; red, *HL*; green, *HF*aT4; blue, *HF*ifx. (A high-quality digital representation of this figure is available in the online issue.)



hypothalamus in a central position in the genesis of diet-induced obesity and suggesting that, at least in this experimental setting, defective hypothalamic regulation of food intake, leading to increased adiposity, precedes whole-body insulin resistance.

Hypothalamic resistance to leptin and insulin can be induced by a number of intracellular mechanisms, such as suppressor of cytokine signaling 3 (SOCS3), protein tyrosine phosphatase 1B (PTP1B), Jun NH2-terminal kinase, inhibitor of nuclear factor kappa kinase (IKK), and endoplasmic reticulum stress (7–10,12). However, it seems that all these intermediates are activated in response to extracellular inflammatory stimuli, where the increased dietary consumption of fatty acids is one of the most relevant of these factors (7). TLR4 signaling induced by dietary saturated fatty acids activates intracellular inflammatory signaling, which leads to the local production of TNF $\alpha$  and other cytokines that act together to boost local inflammation and, thus, lead to insulin and leptin resistance (10).

Here, we hypothesized that the inhibition of TLR4 or TNF $\alpha$  in the hypothalamus would lead to reduced obesity-associated hepatic dysfunction. For this, diet-induced obese rodents were treated intracerebroventricularly with immunoneutralizing antibodies against TLR4 or TNF $\alpha$ . Both approaches, independently, were sufficient to reduce hypothalamic inflammation, as determined by the local expression of cytokines and also by the reduction of hypothalamic resistance to leptin. Of interest, although the inhibition of TLR4 produced some reduction in body mass, TNF $\alpha$  inhibition led to no significant changes in adiposity. These data confirm previous observations (10,18) and suggest that the differences detected between the two approaches may reflect the fact that TLR4 signaling is one of the primary events, if not the prime event, leading to hypothalamic inflammation, whereas TNF $\alpha$  is a downstream phenomenon that contributes to part, but not all, of the inflammatory process.

Subsequently, data show that the inhibition of hypothalamic inflammation by either approach led to an improved insulin signal transduction in the liver but not in the muscle. This finding is in accordance with recent data showing that although the hypothalamic activation of leptin signaling can modulate insulin action in skeletal muscle to

some extent (31), its effect on the inhibition of hepatic glucose production is more pronounced (27).

As expected, the improved insulin signal transduction in the liver was accompanied by a reduction of hepatic steatosis and a reduction of the expression of lipogenic and gluconeogenic enzymes in the liver. Of importance, the hepatic molecular outcomes of the inhibition of hypothalamic inflammation were accompanied by a reduction in glucose production by the liver, as determined by two distinct methods, the pyruvate tolerance test and the hyperinsulinemic-euglycemic clamp. Thus, reducing inflammation-mediated leptin/insulin resistance in the hypothalamus is sufficient to restore the hypothalamus-liver axis that modulates gluconeogenesis.

In the last part of the study, we explored the hypothesis that the liver-damaging signal originated in the inflamed hypothalamus was delivered by the vagus nerve. This hypothesis was based on previous studies, which showed that nutrient- and hormone-induced hypothalamic signals can reach the liver by this route (27). As postulated, in vagotomized rats, all the beneficial effects of the hypothalamic anti-inflammatory approach were hindered. This was further confirmed by the pharmacological inhibition of muscarinic receptors with olanzapine (24).

An additional finding of this study was that, even in the presence of sustained expression of markers of steatosis, in LDL receptor-deficient mice, the inhibition of hypothalamic inflammation still was capable of reducing diet-induced hepatic insulin resistance. This finding has at least two important implications. First, it shows that the cholinergic glucoregulatory route connecting the hypothalamus to the liver is, at least in part, independent of the control of hepatic lipogenesis. Second, it shows that hepatic insulin sensitivity can exist in the presence of a steatotic environment, which can provide new perspectives for the control of gluconeogenesis in obese, diabetic subjects with fatty liver disease.

Thus, the current study expands the current knowledge regarding the existence of a hypothalamus-liver axis, showing its modulation of liver metabolism not only under physiological conditions but also in obesity (27,32). In addition, findings reinforce the important role played by the hypothalamus in obesity, showing that this effect goes much beyond the simple control of food intake and energy expenditure (13,33).

**FIG. 3.** Effect of vagotomy and hepatic steatosis on insulin action in the liver. Intracerebroventricularly cannulated lean rats were treated with 2.0  $\mu$ L saline (L); diet-induced obese rats were treated with 2.0  $\mu$ L saline (HL) or anti-TLR4 antibody (50 ng in 2.0  $\mu$ L [HFaT4]) or anti-TNF $\alpha$  monoclonal antibody infliximab (0.3  $\mu$ g in 2.0  $\mu$ L [HFifx]) twice a day for 7 days. Some diet-induced obese rats were submitted to the surgical procedure for vagotomy, simultaneously with stereotaxic instrumentation (Vtx). In addition, some diet-induced obese rats were submitted to the intraperitoneal treatment with olanzapine (Olz) 0.5 mg/kg twice a day for 7 days, simultaneously with stereotaxic instrumentation. **A:** Histological analysis of liver stained with hematoxylin and eosin, representative of five independent experiments. **B:** The rats were anesthetized and submitted to a venous (cava vein) injection of saline (–) or insulin (+) (100  $\mu$ L,  $10^{-6}$  mol/L). A sample of liver was used for the determination of insulin-induced tyrosine phosphorylation of IR $\beta$  and IRS1 and serine phosphorylation of Akt and FOXO1. IR $\beta$  and IRS1 tyrosine phosphorylation were evaluated in total protein extracts submitted to immunoprecipitation with anti-IR $\beta$  or anti-IRS1 antibodies and immunoblotted with anti-phosphotyrosine antibodies. **C and D:** Blood glucose levels (C) and respective areas under the glucose curve (D) during the pyruvate tolerance test. **E:** Hepatic glucose production during a hyperinsulinemic-euglycemic clamp. **F and G:** PEPCK (F) and G6Pase (G) mRNA levels in liver assessed by real-time PCR in response to vagotomy. **H:** The rats were anesthetized and submitted to a venous (cava vein) injection of saline (–) or insulin (+) (100  $\mu$ L,  $10^{-6}$  mol/L). A sample of liver was used for the determination of insulin-induced tyrosine phosphorylation of IR $\beta$  and IRS1 and serine phosphorylation of Akt. IR $\beta$  and IRS1 tyrosine phosphorylation were evaluated as described above for **B**. **I:** Diet-induced obese mice were used, whereas in **J**, lean, intracerebroventricularly cannulated mice were used. **J:** The mice were either treated intracerebroventricularly with vehicle (V) or stearic acid (SA) 2  $\mu$ L, 90  $\mu$ mol/L twice a day for 5 days. Mice were anesthetized and submitted to a venous (cava vein) injection of saline (–) or insulin (+) (50  $\mu$ L,  $10^{-6}$  mol/L). A sample of liver was used for the determination of insulin-induced tyrosine phosphorylation of IR $\beta$  and IRS1 and serine phosphorylation of Akt. IR $\beta$  and IRS1 tyrosine phosphorylation were evaluated as described above for **B**. **K:** LDL receptor knockout mice were fed a high-fat diet and used for the determination of PGC1 $\alpha$  and PPAR $\alpha$  mRNA levels in liver assessed by real-time PCR. **L:** Mice were anesthetized and submitted to a venous (cava vein) injection of saline (–) or insulin (+) (50  $\mu$ L,  $10^{-6}$  mol/L). A sample of liver was used for the determination of insulin-induced tyrosine phosphorylation of IR $\beta$  and IRS1, as described for **B**. Data are means  $\pm$  SE. In all experiments, \* $P$  < 0.05 vs. lean (L);  $n$  = 5–8 animals. **C:** Black, HF; red, HFaT4Vtx. (A high-quality digital representation of this figure is available in the online issue.)

## ACKNOWLEDGMENTS

This work was supported by grants from the Fundação de Amparo a Pesquisa do Estado de São Paulo. The Laboratory of Cell Signaling belongs to the Instituto Nacional de Ciência e Tecnologia, Obesidade e Diabetes.

No potential conflicts of interest relevant to this article were reported.

M.M. and A.P.A. performed most of the experiments, played important roles in planning and suggesting experiments, and contributed to the statistical analysis and writing of the manuscript. A.C. and L.M.I.-S. conducted the PCR studies. C.E.N., E.A.R., T.R., and L.B.P. contributed to the animal care and conducted the immunoblot studies. A.M.C. conducted the clamp studies. M.A.T. conducted the pyruvate and glucose tolerance tests. P.O.P. and M.J.S. conducted the clamp studies and contributed to the critical reading and writing of the manuscript. L.A.V. contributed to the conception, organization, and writing of the manuscript. L.A.V. is the guarantor of this work and, as such, had full access to all the data in the study and takes responsibility for the integrity of the data and the accuracy of the data analysis.

The authors thank Dr. N. Conran, University of Campinas, for editing the English grammar. The authors also thank Dr. H. Oliveira, University of Campinas, and Dr. J.S. Silva, University of São Paulo, for the kind donation of the LDL receptor knockout and TNFR1 knockout mice, respectively.

## REFERENCES

- Seppälä-Lindroos A, Vehkavaara S, Häkkinen AM, et al. Fat accumulation in the liver is associated with defects in insulin suppression of glucose production and serum free fatty acids independent of obesity in normal men. *J Clin Endocrinol Metab* 2002;87:3023–3028
- Utzhneider KM, Kahn SE. Review: the role of insulin resistance in non-alcoholic fatty liver disease. *J Clin Endocrinol Metab* 2006;91:4753–4761
- Saltiel AR, Kahn CR. Insulin signalling and the regulation of glucose and lipid metabolism. *Nature* 2001;414:799–806
- Hotamisligil GS. Inflammation and metabolic disorders. *Nature* 2006;444:860–867
- Shoelson SE, Lee J, Goldfine AB. Inflammation and insulin resistance. *J Clin Invest* 2006;116:1793–1801
- Foretz M, Hébrard S, Leclerc J, et al. Metformin inhibits hepatic gluconeogenesis in mice independently of the LKB1/AMPK pathway via a decrease in hepatic energy state. *J Clin Invest* 2010;120:2355–2369
- De Souza CT, Araujo EP, Bordin S, et al. Consumption of a fat-rich diet activates a proinflammatory response and induces insulin resistance in the hypothalamus. *Endocrinology* 2005;146:4192–4199
- Howard JK, Cave BJ, Oksanen LJ, Tzameli I, Bjørbaek C, Flier JS. Enhanced leptin sensitivity and attenuation of diet-induced obesity in mice with haploinsufficiency of *Socs3*. *Nat Med* 2004;10:734–738
- Zhang X, Zhang G, Zhang H, Karin M, Bai H, Cai D. Hypothalamic IKK $\beta$ /NF- $\kappa$ B and ER stress link overnutrition to energy imbalance and obesity. *Cell* 2008;135:61–73
- Milanski M, Degasperi G, Coope A, et al. Saturated fatty acids produce an inflammatory response predominantly through the activation of TLR4 signaling in hypothalamus: implications for the pathogenesis of obesity. *J Neurosci* 2009;29:359–370
- Moraes JC, Coope A, Morari J, et al. High-fat diet induces apoptosis of hypothalamic neurons. *PLoS ONE* 2009;4:e5045
- Zabolotny JM, Kim YB, Welsh LA, Kershaw EE, Neel BG, Kahn BB. Protein-tyrosine phosphatase 1B expression is induced by inflammation in vivo. *J Biol Chem* 2008;283:14230–14241
- Kalsbeek A, Bruinstroop E, Yi CX, Klieverik LP, La Fleur SE, Fliers E. Hypothalamic control of energy metabolism via the autonomic nervous system. *Ann N Y Acad Sci* 2010;1212:114–129
- Dzanko N, van Denderen BJ, Hevener AL, et al. AMPK  $\beta$ 1 deletion reduces appetite, preventing obesity and hepatic insulin resistance. *J Biol Chem* 2010;285:115–122
- Purkayastha S, Zhang H, Zhang G, Ahmed Z, Wang Y, Cai D. Neural dysregulation of peripheral insulin action and blood pressure by brain endoplasmic reticulum stress. *Proc Natl Acad Sci USA* 2011;108:2939–2944
- Steinberg GR, Kemp BE. AMPK in health and disease. *Physiol Rev* 2009;89:1025–1078
- Romanatto T, Roman EA, Arruda AP, et al. Deletion of tumor necrosis factor- $\alpha$  receptor 1 (TNFR1) protects against diet-induced obesity by means of increased thermogenesis. *J Biol Chem* 2009;284:36213–36222
- Tsukumo DM, Carvalho-Filho MA, Carvalheira JB, et al. Loss-of-function mutation in Toll-like receptor 4 prevents diet-induced obesity and insulin resistance. *Diabetes* 2007;56:1986–1998
- Ishibashi S, Brown MS, Goldstein JL, Gerard RD, Hammer RE, Herz J. Hypercholesterolemia in low density lipoprotein receptor knockout mice and its reversal by adenovirus-mediated gene delivery. *J Clin Invest* 1993;92:883–893
- Romanatto T, Cesquini M, Amaral ME, et al. TNF- $\alpha$  acts in the hypothalamus inhibiting food intake and increasing the respiratory quotient: effects on leptin and insulin signaling pathways. *Peptides* 2007;28:1050–1058
- Martins EF, Miyasaka CK, Newsholme P, Curi R, Carpinelli AR. Changes of fatty acid composition in incubated rat pancreatic islets. *Diabetes Metab* 2004;30:21–27
- Matthews JN, Altman DG, Campbell MJ, Royston P. Analysis of serial measurements in medical research. *BMJ* 1990;300:230–235
- Prada PO, Zecchin HG, Gasparetti AL, et al. Western diet modulates insulin signaling, c-Jun N-terminal kinase activity, and insulin receptor substrate-1ser307 phosphorylation in a tissue-specific fashion. *Endocrinology* 2005;146:1576–1587
- Weston-Green K, Huang XF, Lian J, Deng C. Effects of olanzapine on muscarinic M3 receptor binding density in the brain relates to weight gain, plasma insulin and metabolic hormone levels. *Eur Neuropsychopharmacol* 6 October 2011 [Epub ahead of print]
- Calegari VC, Torsoni AS, Vanzela EC, et al. Inflammation of the hypothalamus leads to defective pancreatic islet function. *J Biol Chem* 2011;286:12870–12880
- Pocai A, Lam TK, Gutierrez-Juarez R, et al. Hypothalamic K(ATP) channels control hepatic glucose production. *Nature* 2005;434:1026–1031
- German J, Kim F, Schwartz GJ, et al. Hypothalamic leptin signaling regulates hepatic insulin sensitivity via a neurocircuit involving the vagus nerve. *Endocrinology* 2009;150:4502–4511
- Koch C, Augustine RA, Steger J, et al. Leptin rapidly improves glucose homeostasis in obese mice by increasing hypothalamic insulin sensitivity. *J Neurosci* 2010;30:16180–16187
- Thaler JP, Schwartz MW. Minireview: inflammation and obesity pathogenesis: the hypothalamus heats up. *Endocrinology* 2010;151:4109–4115
- Velloso LA, Schwartz MW. Altered hypothalamic function in diet-induced obesity. *Int J Obes (Lond)* 2011;35:1455–1465
- Roman EA, Reis D, Romanatto T, et al. Central leptin action improves skeletal muscle AKT, AMPK, and PGC1  $\alpha$  activation by hypothalamic PI3K-dependent mechanism. *Mol Cell Endocrinol* 2010;314:62–69
- Buettner C, Camacho RC. Hypothalamic control of hepatic glucose production and its potential role in insulin resistance. *Endocrinol Metab Clin North Am* 2008;37:825–840
- Obici S, Rossetti L. Minireview: nutrient sensing and the regulation of insulin action and energy balance. *Endocrinology* 2003;144:5172–5178